Review

Bond Strength—Coordination Number Fluctuation Model of Viscosity: An Alternative Model for the Vogel-Fulcher-Tammann Equation and an Application to Bulk Metallic Glass Forming Liquids

Masahiro Ikeda [1],* and Masaru Aniya [2]

[1] Course of General Education, Natural Science, Fukui National College of Technology, Geshi-chou, Sabae, Fukui 916-8507, Japan

[2] Department of Physics, Graduate School of Science and Technology, Kumamoto University, Kumamoto 860-8555, Japan; E-Mail: aniya@gpo.kumamoto-u.ac.jp

* Author to whom correspondence should be addressed; E-Mail: mikeda@fukui-nct.ac.jp; Tel.: +81-778-62-8228; Fax: +81-778-62-2597.

Abstract: The Vogel-Fulcher-Tammann (VFT) equation has been used extensively in the analysis of the experimental data of temperature dependence of the viscosity or of the relaxation time in various types of supercooled liquids including metallic glass forming materials. In this article, it is shown that our model of viscosity, the Bond Strength—Coordination Number Fluctuation (BSCNF) model, can be used as an alternative model for the VFT equation. Using the BSCNF model, it was found that when the normalized bond strength and coordination number fluctuations of the structural units are equal, the viscosity behaviors described by both become identical. From this finding, an analytical expression that connects the parameters of the BSCNF model to the ideal glass transition temperature T_0 of the VFT equation is obtained. The physical picture of the Kohlrausch-Williams-Watts relaxation function in the glass forming liquids is also discussed in terms of the cooperativity of the structural units that form the melt. An example of the application of the model is shown for metallic glass forming liquids.

1. Introduction

The Vogel-Fulcher-Tammann (VFT) equation [1-3] is one of the most commonly used expressions for the analysis of the temperature dependence of viscosity [4-9], relaxation time [5,8,10,11], diffusion coefficient [5-7,9], and electrical conductivity [5-7], *etc*. The application of the VFT equation covers a wide field of research [12]. It has been reported that the transport properties of supercooled melts can change at certain characteristic temperatures such as the dynamical crossover temperature T_c [8,11,13,14]. By reducing the temperature of the liquid below T_c, the thermally activated hopping process becomes dominant [15]. In such a process, the activation energy for the transport properties is often discussed in the frame of the Arrhenius law expressed as $A = A_0 \exp(\pm E_a/RT)$, where A, A_0, R and E_a denote the transport coefficient, its pre-exponential factor, the gas constant, and the activation energy for the transport coefficient, respectively. In this case, the activation energy E_a is considered as the energy barrier that the mobile species, such as ions or molecules, must overcome to move from one position to another. However, in most cases, the value of E_a is not a constant [16-18] and changes with variation in temperature. Some studies have shown that the variations of the activation energy for the transport properties are affected by their diffusion and structural relaxation mechanism during supercooling [5,8,9,13,16,17,19].

According to the strong-fragile classification of glass forming liquids [13,20,21], systems obeying the Arrhenius law are called strong system. These systems exhibit an almost straight line in the temperature dependence of the viscosity when plotted against the inverse temperature normalized by their glass transition temperature T_g/T. Such a plot is usually called Angell's plot. On the other hand, systems showing a large curvature in the temperature dependence do not follow the Arrhenius law, due to changes of the activation energy E_a that apparently depends on temperature [16-19]. Such systems are called fragile system. To describe the behavior observed in fragile systems, the VFT equation has often been employed [4,6,7]. Although the physical background of the VFT equation has been fully discussed from the theoretical point of view [10,22], there might be some discrepancies between the experimental data and its interpretation when the actual data and the VFT equation are compared. The VFT equation has been used as a practical equation to reproduce the experimental data, and therefore it is not sufficient to understand the physics behind the glass forming process. For instance, one of the parameters of the VFT equation, the so-called ideal glass transition temperature T_0 which indicates the dynamical divergence in the temperature dependence of the viscosity or relaxation time, is not observed in real systems [18]. Another point is that the values of the parameters of the VFT equation, obtained from the data analysis, have not been fully exploited. Specifically, although the VFT equation reproduces the experimental data, no concrete microscopic physical picture of the melt and further knowledge on the structural relaxation can be extracted from the VFT parameters alone.

Previously, a model for temperature dependence of the viscosity of melt has been proposed by one of the authors [23]. The model which is called Bond Strength—Coordination Number Fluctuation (BSCNF) model, describes the viscosity behavior in terms of the mean values of the bond strength E_0, the coordination number Z_0, and their fluctuations, ΔE, ΔZ, of the structural units that form the melt. In our previous works, the model has been applied to investigate the viscosity of many kinds of glass forming liquids such as covalent, ionic, molecular, metallic, and polymeric materials [24-27]. It has been shown that the model reproduces experimental data well, and characterizes many kinds of glass forming liquids extending from strong to fragile systems. From the theoretical side, it has also been

shown that the viscous flow is accompanied by cooperatively rearranging movements of the structural units and occurs by breaking selectively weaker parts of the bonds [24,28]. This notion of the viscous flow is closely related to the well-known concept to explain the glass transition phenomena, the "cooperatively rearranging region (CRR)" as proposed by Adam and Gibbs [29]. Thus, our model of the thermally activated viscous flow, provides further understanding of the structural relaxation, in addition to other well-known theories such as the configurational entropy theory [29-31], the free volume theory [32,33], and to the picture obtained from the activated volume [34], *etc*.

In this article, it is shown that under certain conditions, the BSCNF model reproduces exactly the same viscosity behavior as the VFT equation [25,26,35]. The prerequisite is that the normalized bond strength fluctuation $|\Delta E|/E_0$ equals the normalized coordination number fluctuation $|\Delta Z|/Z_0$. This condition makes it possible to directly connect the parameters of the VFT equation, such as the ideal glass transition temperature T_0, to the parameters of the BSCNF model, which contain microscopic information related to bonding connectivity among the constituent elements. Thus, the BSCNF model incorporates the VFT relation. By choosing the best fitting parameters, it reproduces the experimental data better than the VFT equation. In this review, the correlation between the fragility index of various glass forming liquids and the stretched exponent of the Kohlrausch-Williams-Watts (KWW) relaxation function [36,37], is also discussed in terms of the cooperativity which is defined by the BSCNF model.

2. The BSCNF Model and the VFT Equation

Commonly, glasses are formed by quenching a liquid. In the course of lowering the temperature, the value of the viscosity increases drastically reaching approximately 10^{12} Pa s at the glass transition temperature T_g. At the microscopic scale, the constituent elements of the glasses are considered to form certain types of clusters or structural units. Such structural units are bound to others by a certain bond strength retaining its spatial random connectivity. Within the glass-forming liquid, thermally activated viscous flow occurs due to bond-breaking and bond-switching. In addition, it must be noted that it is not necessary to break all the bonds connecting to the nearest neighbor components when the thermally activated viscous flow occurs. Bond twisting may also result in the viscous flow by enrolling the movement of second or more distant components of the melt.

Based on this picture, a model for the temperature dependence of the viscosity, the Bond Strength—Coordination Number Fluctuation (BSCNF) model, has been proposed by one of the authors [23]. The BSCNF model is given by

$$\eta = \frac{\eta_0}{\sqrt{1 - Bx^2}} \exp\left[\frac{Cx + Cx^2\left[\left\{ \ln\left(\frac{\eta_{Tg}}{\eta_0}\right) + \frac{1}{2}\ln(1 - B) \right\} \frac{(1 - B)}{C} - 1 \right]}{1 - Bx^2} \right], \tag{1}$$
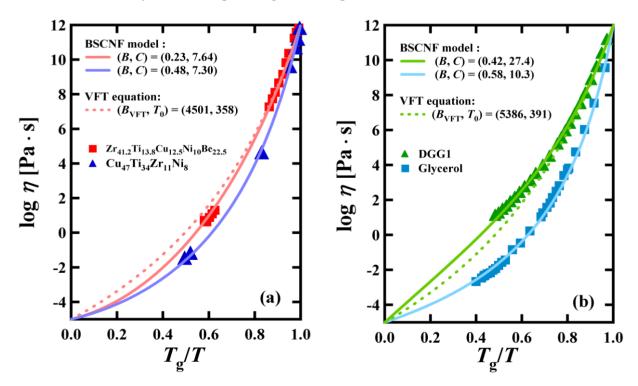
where

$$B = \frac{(\Delta E)^2 (\Delta Z)^2}{R^2 T_g^2}, \quad \text{and} \quad C = \frac{E_0 Z_0}{RT_g}. \tag{2}$$

Here, x is the inverse temperature normalized by T_g, $x = T_g/T$. R is the gas constant. η_0 and η_{Tg} are the viscosity at the high temperature limit and at the glass transition temperature, respectively. The fitting parameters B and C defined in Equation 2 have the following intuitive meanings: C gives the mean total binding energy per structural unit and B gives the degree of its fluctuations among the structural units against the thermal disturbance at T_g. Regarding the number of parameters, the BSCNF model given in Equation 1 has five fitting parameters, namely, B, C, η_{Tg}, η_0, and T_g. However, it must be noted that the effect of T_g is embodied in B and C as given in Equation 2. Thus, in the case where the viscosity is plotted in the Angell's plot, the BSCNF model given in Equation 1 has four fitting parameters, *i.e.*, B, C, η_{Tg}, and η_0.

Figure 1 shows some applications of the BSCNF model. The viscosity of bulk metallic glass forming liquids such as $Zr_{41}Ti_{13.8}Cu_{12.5}Ni_{10}Be_{22.5}$ and $Cu_{47}Ti_{34}Zr_{11}Ni_8$, and other type of materials such as DGG1 (a kind of soda lime silicate glass) and Glycerol, are shown in Figure 1 (a) and (b), respectively. As can be seen in these figures, the BSCNF model reproduces the viscosity data better than the VFT equation.

Figure 1. (a) Temperature dependence of the viscosity in bulk metallic glass forming liquids ($Zr_{41}Ti_{13.8}Cu_{12.5}Ni_{10}Be_{22.5}$ and $Cu_{47}Ti_{34}Zr_{11}Ni_8$); and (b) DGG1 (Soda lime silicate glass) and Glycerol. The data shown with the symbols are taken from the reference [38] in (a) and reference [39] in (b). The full lines are reproduced by the BSCNF model, and the dashed lines are by the VFT equation given in Equation 5.

According to the BSCNF model, glass forming liquids are characterized by the set of parameters B and C [23,24]. Figure 2 shows that many kinds of glass forming materials, including covalent, metallic, and molecular glassy systems, are characterized in a mapping plotted in the B-C space. From this figure, we note an interesting trend. Strong system is characterized by a large value of C and a small

value of *B*. While, fragile system is characterized by a small value of *C* and a large value of *B*. In this manner, the BSCNF model can characterize any kind of glass forming material in terms of *B* and *C*, or, E_0, Z_0, ΔE, and ΔZ. It is expected that the characteristics of glass forming materials are reflected through these quantities. Furthermore, by studying the trend, we note that there is a correlation between *B* and *C*, which has been suggested in our previous work [24]. Such a correlation is shown by the shaded area in Figure 2. It has also been found that an analytical relation, reproducing this correlation between *B* and *C*, can be derived from the BSCNF model [28]. The relation is given by

$$C = \frac{2\gamma(1-B)}{2\gamma + \sqrt{B}(1+\gamma^2)}\left\{\ln\left(\frac{\eta_{Tg}}{\eta_0}\right) + \frac{1}{2}\ln(1-B)\right\}, \tag{3}$$

where

$$\gamma = \frac{|\Delta E|/E_0}{|\Delta Z|/Z_0}. \tag{4}$$

Note that γ gives the ratio of the normalized bond strength fluctuation to the normalized coordination number fluctuation. The dashed line in Figure 2 shows the behavior given by Equation 3 for the case of $\gamma = 1$ with $\eta_{Tg} = 10^{12}$ Pa s and $\eta_0 = 10^{-5}$ Pa s. In one of our previous works, the composition and temperature dependence of the viscosity in $Cu_x(As_2Se_3)_{1-x}$ ($x \leq 0.20$) was discussed [28]. There, it was shown that in this system, the ratio of the fluctuations γ can take relatively large values, $\gamma \approx 15$. The result suggests that for the Cu-As-Se system, there is a strong composition dependence in the bond strength fluctuation and a weak dependence in the coordination number fluctuation and fragility.

Furthermore, we have compared and discussed the interrelation between the VFT equation and the BSCNF model [25,26]. It has been found that in the case of $\gamma = 1$, the viscosity behavior described by Equation 1 with the set of parameters (*B*, *C*) obeying the relation Equation 3, perfectly follows the behavior described by the VFT equation,
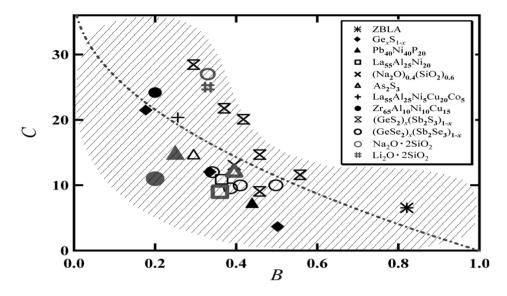
$$\log\eta = A_{\text{VFT}} + \frac{B_{\text{VFT}}}{T - T_0}, \tag{5}$$

where A_{VFT} is the logarithm of the viscosity at the high temperature limit, $A_{\text{VFT}} = \log\eta_0$, and B_{VFT}, T_0 are the free fitting parameters of the VFT equation. It is considered that at the ideal glass transition temperature T_0, which is also called "Vogel temperature", the movement of the atoms is totally frozen. In the VFT equation, the number of fitting parameters is three, namely, B_{VFT}, T_0, and η_0. One of the reasons that the BSCNF model reproduces the experimental data better than the VFT equation, as shown in Figure 1, is due to the difference in the number of free parameters. Here, it should be noted that for the case of $\gamma = 1$, the number of free parameters of the BSCNF model reduces from four to three, *B*, η_{Tg}, and η_0, because *C* and *B* are connected mutually through Equation 3.

At the glass transition temperature, the VFT equation given by Equation 5 reduces to

$$\ln\left(\frac{\eta_{Tg}}{\eta_0}\right) = \frac{\ln(10)\left(\dfrac{B_{\text{VFT}}}{T_g}\right)}{1 - \left(\dfrac{T_0}{T_g}\right)}. \tag{6}$$

Figure 2. Mapping of different kinds of glass-forming liquids in the *B-C* space. The dashed curve indicates Equation 3 for the case of $\gamma = 1$ with $\eta_{Tg} = 10^{12}$ Pa·s and $\eta_0 = 10^{-5}$ Pa·s. The correlation between *B* and *C* that has been suggested previously [24] is shown by shaded area.

In Table 1, the key parameters for 38 kinds of oxide glass forming materials are indicated. In order to check the exact fitting between the VFT equation and the BSCNF model, in this analysis, we used the collection of fitting parameters by the VFT equation given in reference [4], where the values of B_{VFT}, T_0, T_g, and the fragility index *m* for various oxide glass forming materials are provided. The numerical values of both, $\ln(\eta_{Tg}/\eta_0)$ calculated by Equation 6, and the best fitting parameters (B^*, C^*) determined by the BSCNF model, are also indicated in Table 1.

The fragility index *m* is defined as $m = \mathrm{d}\log\eta/\mathrm{d}\,(T_g/T)|_{T=Tg}$ [21]. From the BSCNF model of the viscosity given in Equation 1, we obtain the fragility index *m* [23-26].

$$m = \frac{1}{\ln(10)}\left\{\frac{B - C + 2\left[\ln\left(\dfrac{\eta_{Tg}}{\eta_0}\right) + \dfrac{1}{2}\ln(1 - B)\right]}{1 - B}\right\}. \tag{7}$$

On the other hand, from the VFT equation given in Equation 5, we obtain another fragility expression,

$$m = \frac{\left(\dfrac{B_{VFT}}{T_g}\right)}{\left\{1 - \left(\dfrac{T_0}{T_g}\right)\right\}^2}. \tag{8}$$

Table 1. Parameters of various oxide glass forming materials. Data of B_{VFT}, T_0, T_g, and m are taken from reference [4]. The values of $\ln(\eta_{Tg}/\eta_0)$, and the best fitted parameters (B^*, C^*), are calculated from Equations 1, 3 and 7 under the condition that Equation 3 satisfies $\gamma = 1$.
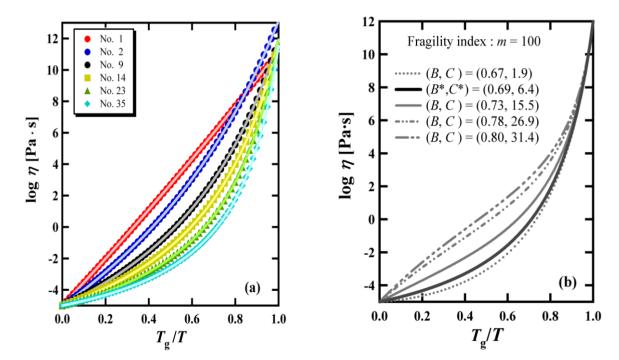
No.	Material	B_{VFT} (K)	T_0 (K)	T_g (K)	m	$\ln(\eta_{Tg}/\eta_0)$	(B^*, C^*)
1.	SiO_2	21,254	139	1,450	17.9	37.3	(0.01, 3.8)
2.	$Li_2O\ SiO_2$	5,744	276	593	33.9	41.7	(0.22, 2.3)
3.	$Li_2O\ 2SiO_2$	5,752	380	727	34.7	38.2	(0.27, 18.2)
4.	$Li_2O\ 3SiO_2$	8,218	255	734	26.3	39.5	(0.12, 25.7)
5.	$Na_2O\ SiO_2$	4,999	395	687	40.3	39.4	(0.33, 16.7)
6.	$Na_2O\ 2SiO_2$	5,538	393	728	35.9	38.1	(0.23, 17.5)
7.	$Na_2O\ 3SiO_2$	7,484	287	743	26.7	37.8	(0.15, 23.2)
8.	$Na_2O\ 4SiO_2$	7,618	323	765	29.8	39.7	(0.18, 22.9)
9.	$K_2O\ SiO_2$	4,395	416	675	44.2	39.1	(0.38, 14.9)
10.	$K_2O\ 2SiO_2$	7,461	333	768	30.3	39.5	(0.19, 22.3)
11.	$K_2O\ 3SiO_2$	8,334	253	760	24.6	37.9	(0.11, 25.3)
12.	$K_2O\ 4SiO_2$	8,471	255	766	24.8	38.2	(0.11, 25.5)
13.	$Na_2O\ Al_2O_3\ 6SiO_2$	12,281	347	1,087	24.4	38.2	(0.10, 26.0)
14.	$CaO\ MgO\ 2SiO_2$	4,826	710	995	59.1	39.0	(0.51, 11.1)
15.	$CaO\ Al_2O_3\ 2SiO_2$	5,802	785	1,113	60.0	40.7	(0.50, 11.9)
16.	$2MgO\ 2Al_2O_3\ 5SiO_2$	8,244	583	1,088	35.2	37.6	(0.29, 17.4)
17.	$15.45Na_2O\ 12.81CaO\ 71.74SiO_2$	6,785	421	819	35.1	39.3	(0.26, 19.0)
18.	$2BaO\ TiO_2\ 2SiO_2$	3,896	750	983	70.5	38.5	(0.58, 9.0)
19.	$PbO\ SiO_2$	3,690	454	673	51.8	38.8	(0.46, 12.5)
20.	$PbO\ 2SiO_2$	6,001	390	749	34.9	38.5	(0.27, 18.4)
21.	$2PbO\ SiO_2$	2,496	473	613	78.1	41.1	(0.60, 9.2)
22.	B_2O_3	4,695	252	540	30.6	37.5	(0.22, 20.0)
23.	$Li_2O\ B_2O_3$	2,557	542	693	77.7	39.0	(0.61, 8.4)
24.	$Li_2O\ 2B_2O_3$	2,497	616	763	88.2	39.1	(0.65, 7.4)
25.	$Li_2O\ 3B_2O_3$	2,850	598	768	76.6	38.8	(0.61, 8.4)
26.	$Li_2O\ 4B_2O_3$	2,908	579	751	73.8	38.9	(0.60, 8.8)
27.	$Na_2O\ 2B_2O_3$	2,405	600	748	82.1	37.4	(0.65, 7.3)
28.	$Na_2O\ 3B_2O_3$	3,121	557	746	65.2	38.0	(0.56, 9.5)
29.	$Na_2O\ 4B_2O_3$	3,172	539	727	65.2	38.9	(0.55, 9.9)
30.	$K_2O\ 2B_2O_3$	2,888	520	705	59.5	36.0	(0.55, 9.3)
31.	$K_2O\ 3B_2O_3$	3,403	512	709	62.2	39.8	(0.52, 10.9)
32.	$K_2O\ 4B_2O_3$	3,588	463	691	47.7	36.2	(0.45, 11.9)
33.	$Cs_2O\ 3B_2O_3$	3,363	491	693	57.1	38.3	(0.50, 11.1)
34.	$BaO\ 2B_2O_3$	3,262	619	810	72.4	39.3	(0.59, 9.2)
35.	$SrO\ 2B_2O_3$	2,592	755	911	97.0	38.3	(0.69, 6.4)
36.	$PbO\ B_2O_3$	2,171	525	658	80.8	37.6	(0.64, 7.5)
37.	$PbO\ 2B_2O_3$	3,020	545	738	59.8	36.0	(0.55, 9.3)
38.	$PbO\ 3B_2O_3$	2,656	569	728	76.5	38.5	(0.61, 8.3)

3. Comparison between the BSCNF Model and the VFT Equation

Figure 3 (a) shows the complete correspondence of the viscosity behaviors reproduced by the VFT equation and the BSCNF model. In Figure 4, we can see that all the materials given in Table 1 are located on the curve $C(B, \gamma = 1)$ described by Equation 3 in the *B-C* space. This result provides a physical interpretation to the VFT relation, from the BSCNF model's point of view. Specifically, according to the BSCNF model, the glass forming liquids whose viscosity data are described by the VFT equation satisfies the following relation [35],

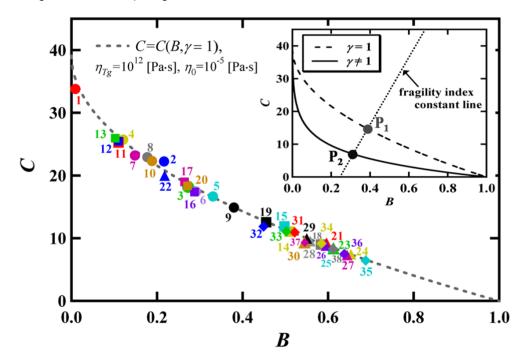$$\frac{|\Delta E|}{E_0} = \frac{|\Delta Z|}{Z_0}. \tag{9}$$

Figure 3. (a) The exact correspondence between the temperature dependence of viscosity described by the VFT equation (symbols) and that described by the BSCNF model (solid lines). The materials numbers are the same as given in Table 1. (b) The viscosity behaviors described by Equation 1 with five different values of (B, C). B^* and C^* indicate the value of B and C that perfectly reproduces the VFT behavior.

The physical meaning given by Equation 9 is clearer than that of the fitting parameters used in the VFT equation, because, for instance, the ideal glass transition temperature T_0, which indicates the dynamical divergence in the temperature dependence of the viscosity or relaxation time, is not directly observed [18]. The quantities E_0, Z_0, and ΔE, ΔZ used in Equation 9 are in principle measurable quantities. It should be mentioned, however, that the theoretical justification of the derivation of the VFT equation from the BSCNF model, by imposing the condition given in Equation 9, remains to be solved. In Figure 2, it is shown that not all the materials are located on the curve of $C(B, \gamma = 1)$. This result indicates that for different glass forming materials, the distribution of the connectivity among the structural units which is described by E and Z differs among the glassy materials. In the inset of Figure 4,

it is shown that $C(B, \gamma \neq 1)$ deviates from $C(B, \gamma = 1)$ When the set of values (B, C) at P_1 is used, for instance, Equation 1 reproduces exactly the viscosity behavior described by the VFT equation as shown in Figure 3 (a). Thus, by changing (B, C), the BSCNF model can reproduce the experimental behavior better than the VFT equation. Such a set of values (B, C) is denoted schematically by P_2 which is on the line of $C(B, \gamma \neq 1)$ in the inset. Figure 3 (b) shows the different viscosity behaviors described by Equation 1 with five different sets of (B, C). Here, (B^*, C^*) exactly reproduces the behavior given by the VFT equation. As noted above, by changing (B, C), the experimental data of the viscosity from strong to fragile glass forming systems are well reproduced. However, analogous to the case of the VFT equation [8,16,40], in some cases such as the van der Waals liquids [41] and metallic glass forming systems [42], the BSCNF model does not reproduce the experimental data over a wide temperature range. This is due to the fact that in the high temperature region above T_g, a salient change in the transport properties emerges near the dynamical crossover temperature T_c as predicted by the widely discussed mode-coupling theory [5,8,13,14].

Figure 4. The viscosity described by Equation 1 using the set of parameters (B^*, C^*) that satisfy Equation 3 with $\gamma = 1$ corresponds exactly to that described by the VFT equation given in Equation 5. The γ dependence is illustrated in the inset.

Using Equations 3, 6, and 8, the following relation that analytically connects the parameters of the VFT equation, T_0, with that of the BSCNF model, B and C, is obtained,

$$\frac{T_0}{T_g} = 1 - \frac{\left(\dfrac{1+\sqrt{B^*}}{1-B^*}\right)C^* - \dfrac{1}{2}\ln(1-B^*)}{\ln(10)\,m} \quad , \tag{10}$$

where B^* and C^* denote the values of B and C that satisfy Equation 3 in the case of $\gamma = 1$. It is noteworthy that B^* and C^* are calculated as a function of the fragility index m. In the inset of Figure 4,

the point P_1 is designated as (B^*, C^*) and denotes the intersection between the line of constant fragility index m with the curve $C(B, \gamma = 1)$ given by Equation 3. In other words, if the value of fragility index m is given, the set of (B^*, C^*) can be determined uniquely by calculating the intersection. The applicability of Equation 10 has been discussed by applying it to some polymeric [25] and metallic materials [27]. The characteristic temperature ratio T_0/T_g, is related to the fragility [14,19,43-45]. While, by using the VFT equation, another expression for the characteristic temperature ratio T_0/T_g is derived

$$\frac{T_0}{T_g} = \frac{\ln\left(\dfrac{\eta_{T_g}}{\eta_0}\right)}{D + \ln\left(\dfrac{\eta_{T_g}}{\eta_0}\right)} \,, \tag{11}$$

or by using the fragility index m, we also have

$$\frac{T_0}{T_g} = \left\{1 + \frac{D}{2m}\right\} - \sqrt{\left(\frac{D}{m}\right)\left\{\frac{1}{4}\left(\frac{D}{m}\right) + 1\right\}}, \tag{12}$$

where, D is the strength parameter defined as $D = B_{VFT}/T_0$ [45,46]. The expressions for T_0/T_g given in the above equations have been used, for instance, in the analysis of pressure dependence of relaxation behavior of supercooled liquids [43]. Here, it must be noted that T_0/T_g can be used as an index equivalent to the fragility, because the ratio takes values between 0 (the strongest) and 1 (the most fragile) [46]. The same statement applies to the expression given in Equation 10. For the case of strong systems, such as SiO_2, B^* is nearly 0, and C^* takes approximately $C^* \approx 39.1$. Thus, the right hand side of Equation 10 equals nearly 0, because for this system $m \approx 17$. On the other hand, in more fragile systems, B^* and C^* take a larger and a smaller values, respectively. In such a case the value of T_0/T_g given by Equation 10 approaches unity. Therefore, the information on bonding of the structural units is embodied in T_0/T_g, and is described in terms of the parameters of the BSCNF model by using the expression given in Equation 10. It was concluded in reference [18] that the prediction by the VFT equation with dynamic divergence at T_0 lacks direct experimental evidences. Their experimental investigations indicate that a simple use of the VFT equation is not sufficient to fully understand the physics of glass transition phenomena behind structural relaxation. So far, quite a large number of studies regarding the VFT equation have been accumulated. By linking these large numbers of works with the result obtained from the BSCNF model, especially by using Equation 10, it is expected that further knowledge on structural relaxation in glass forming melt can be extracted.

4. Correlation between the Exponent of the KWW Function and the Fragility

Many physical quantities exhibit a universal feature in their structural relaxation behaviors which mainly involve the cooperative relaxation motions of the constituent elements toward the glass transition. To describe such a behavior, the Kohlrausch-Williams-Watts (KWW) function [36,37] has been widely used [5,8,10,17,33,40,47-50]. It is written as

$$\phi_{\mathrm{KWW}}(t) = \phi_0 \exp\left[-\left(\frac{t}{\tau}\right)^{\beta_{\mathrm{KWW}}}\right], \qquad 0 < \beta_{\mathrm{KWW}} \leq 1, \tag{13}$$

where ϕ_0 is the value of the physical quantity at time $t = 0$. β_{KWW} is the exponent of the KWW function which is called "stretched exponent", and τ is the structural relaxation time.

It is widely accepted that β_{KWW} gives the degree of many-body interactions among the constituent elements of structurally disordered materials [33,40,50]. It is known that in the case of $\beta_{\mathrm{KWW}} = 1$, structural relaxation reduces to the Debye relaxation where all the elements of the glass exhibit a simple relaxation. For systems characterized by a small value of β_{KWW}, on the other hand, many modes of relaxation are present, leading to non-linear relaxation [10,33]. It is also known that β_{KWW} is related to the fragility and that the non-linear relaxation behaviors are related to the α-relaxation described by the VFT equation [10,21].

According to Vilgis [51], the stretched exponent β_{KWW} and the strength parameter D are mutually connected through the following relation
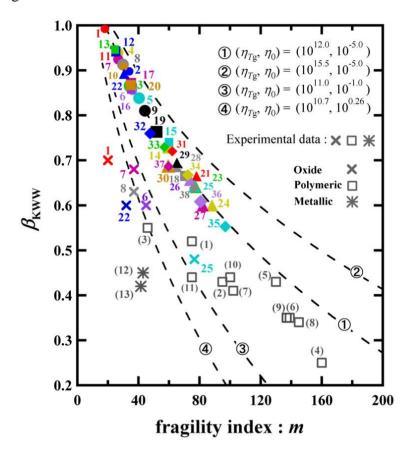
$$\beta_{\mathrm{KWW}} = 1 - \sqrt{\frac{(T_0/T_g)^2}{D}} \ . \tag{14}$$

Equation 14 is used to check the value of β_{KWW} with the VFT equation [45,52]. Using this relation together with Equation 8, the following relation between the stretched exponent β_{KWW}, the characteristic temperature ratio T_0/T_g, and the fragility index m is obtained,

$$\beta_{\mathrm{KWW}} = 1 - \frac{(T_0/T_g)}{1 - (T_0/T_g)}\sqrt{\frac{(T_0/T_g)}{m}} \ . \tag{15}$$

In Figure 5, the relation between the exponent of the KWW function and the fragility index is shown. The symbols used in Figure 5 are the same as those used in Figure 4. The values of β_{KWW} are calculated from Equation 15. The dashed curves in Figure 5 are calculated from Equation 15 with T_0/T_g given in Equation 10. We can see that all values of β_{KWW} for the materials indicated in Table 1 follow the theoretical curve when $\eta_{Tg} = 10^{12}$ Pa·s and $\eta_0 = 10^{-5}$ Pa·s are used. A correlation between the fragility index m and β_{KWW} has been observed in many kinds of glass-forming liquids [17,21,48,49]. It is expressed as $m = C_1 - C_2\beta_{\mathrm{KWW}}$, where C_1 and C_2 are constants [21]. This phenomenological relation is analogous to our result shown in Figure 5. It must be noted however that for some glassy materials, the data measured do not necessarily follow the theoretical curve calculated with $\eta_{Tg} = 10^{12}$ Pa·s and $\eta_0 = 10^{-5}$ Pa·s. In Figure 5, other theoretical curves calculated by using different values of η_{Tg} and η_0 are also shown. The same approach has been employed for many types of bulk metallic systems [27]. Although the validity of Equation 10 is restricted to the case of $\gamma = 1$, the result of Figure 5 provides a sound physical meaning of β_{KWW} in respect to the BSCNF model.

Figure 5. Relation between the exponent of KWW function and the fragility index. The dashed curves are calculated from Equation 15 with T_0/T_g given in Equation 10 by varying the values of η_{Tg} and η_0. The colored symbols are the same as those used in Figure 4. Actual values determined by experiments are also indicated. The experimental data shown in this figure are given in Table 2.

Previously, a quantity defined as $N_B = E_\eta /(E_0 Z_0)$ which gives the number of structural units involved in the thermally activated viscous flow has been introduced in the framework of the BSCNF model [24]. Here, E_η denotes the activation energy for the viscous flow. It has been shown that N_B can be expressed analytically by B and C, $N_B(B,C)$ at T_g, and the value of N_B increases with the increase in the fragility index m [28]. From the results, it was suggested that the thermally activated viscous flow occurs when the weaker parts of bonds are selectively broken. This observation indicates that systems with a smaller value of β_{KWW} correspond to systems that have a larger value of N_B. In this regard, some researchers have reported similar ideas. For instance, Park *et al*. have mentioned that the non-exponentiality given by β_{KWW} is directly affected by the intermolecular cooperativity, resulting in the increase of the domain size of the glass-forming alcohols [10]. Similarly, Rault has indicated that the connection between cooperative motion of α-relaxation and β_{KWW} leads to the VFT law [53]. This picture of the cooperativity gained through the quantity N_B is also in harmony with the concepts proposed by others such as the "cooperativity of atomic migrations" given by Wang and Fecht [54], and the "supercooled liquid as an elastic medium" given by Trachenko [55,56], *etc*. Our view of the cooperativity gives the same result and provides an alternative view to understand the structural relaxation, that is, in terms of the structural units which is determined by the bonding nature. All these results indicate that the BSCNF model could be an alternative to the VFT equation which has been

widely used in the analysis of the temperature dependence of the viscosity. The BSCNF model provides a clearer physical picture and microscopic information on bonding and cooperativity of the constituent elements within the viscous liquids.

Table 2. Experimental values of the stretched exponent β_{KWW} and the fragility index m for some materials such as oxide, polymeric, and metallic systems.

	Materials	m	β_{KWW}	Reference
1.	SiO_2	20	0.70	[21]
6.	$Na_2O\ 2SiO_2$	45	0.60	
7.	$Na_2O\ 3SiO_2$	37	0.68	
8.	$Na_2O\ 4SiO_2$	37	0.63	
22.	B_2O_3	32	0.60	
25.	$Li_2O\ 3\ B_2O_3$	77	0.48	[47]
(1)	Poly(propylene glycol)	75	0.52	[17]
(2)	Poly(vinyl acetate)	95	0.43	
(3)	Polyisobutylene	46	0.55	[57]
(4)	Polyvinyle chloride	160	0.25	
(5)	Polyvinyl acetate	130	0.43	
(6)	Polystyrene	139	0.35	
(7)	Polymethyl acrylate	102	0.41	
(8)	Poly(methylmethacrylate)	145	0.34	[21]
(9)	Polypropylene	137	0.35	
(10)	Poly(methylphenysiloxane)	100	0.44	
(11)	Poly(vinylmethylether)	75	0.44	
(12)	$Zr_{65}Al_{7.5}Cu_{17.5}Ni_{10}$	43	0.45	[48]
(13)	$Pd_{40}Ni_{40}P_{20}$	42	0.42	

5. Conclusions

In this paper, the BSCNF model has been reviewed. In particular, it was shown that in the case where the magnitudes of energy and coordination number fluctuations of the structural units are equal, the viscosity behavior described by the BSCNF model corresponds perfectly to that described by the VFT equation. It was also shown that the characteristic temperatures ratio T_0/T_g can be expressed in terms of the parameters of the BSCNF model, namely, the total bond strength, average coordination number and their fluctuations of the structural units, leading to a new way to understand the cooperativity of the structural relaxation in supercooled liquids. Furthermore, by connecting the BSCNF model with another model given by Vilgis, a theoretical relation that correlates the stretched exponent of the KWW function β_{KWW}, and the fragility index m has been obtained.

Acknowledgements

References

1. Vogel, H. The law of relation between the viscosity of liquids and the temperature. *Phys. Z* **1921**, *22*, 645-646.

2. Fulcher, G.S. Analysis of recent measurements of viscosity of glasses. *J. Amer. Ceram. Soc.* **1925**, *8*, 339-355.

3. Tammann, G.; Hesse, W. The dependence of viscosity upon the temperature of supercooled liquids. *Z. Anorg. Allg. Chem.* **1926**, *156*, 245-257.

4. Nascimento, M.L.F.; Aparicio, C. Viscosity of strong and fragile glass-forming liquids investigated by means of principal component analysis. *J. Phys. Chem. Solids* **2007**, *68*, 104-110.

5. Stickel, F.; Fischer, E.W.; Richert, R. Dynamics of glass-forming liquids. II. Detailed comparison of dielectric relaxation, dc-conductivity, and viscosity data. *J. Chem. Phys.* **1996**, *104*, 2043-2055.

6. Noda, A.; Hayamizu, K.; Watanabe, M. Pulsed-Gradient Spin-Echo ^{1}H and ^{19}F NMR ionic diffusion coefficient, viscosity, and ionic conductivity of non-chloroaluminate room-temperature ionic liquids. *J. Phys. Chem. B* **2001**, *105*, 4603-4610.

7. Tokuda, H.; Hayamizu, K.; Ishii, K.; Susan, M.A.B.H.; Watanabe, M. Physicochemical properties and structures of room temperature ionic liquids. 1. Variation of anionic species. *J. Phys. Chem. B* **2004**, *108*, 16593-16600.

8. Stickel, F.; Fischer, E.W.; Richert, R. Dynamics of glass-forming liquids. I. Temperature-derivative analysis of dielectric relaxation data. *J. Chem. Phys.* **1995**, *102*, 6251-6257.

9. Rössler, E. Indications for a change of diffusion mechanism in supercooled liquids. *Phys. Rev. Lett.* **1990**, *65*, 1595-1598.

10. Park, I.-S.; Saruta, K.; Kojima, S. Dielectric relaxation and calorimetric measurements of glass transition in the glass-forming dyhydroxyl alcohols. *J. Phys. Soc. Jpn.* **1998**, *67*, 4131-4138.

11. Nozaki, R.; Zenitani, H.; Minoguchi, A.; Kitai, K. Dielectric relaxation processes in water-in-sorbitol mixtures. *J. Non-Cryst. Solids* **2002**, *307-310*, 349-355.

12. Liu, H.; Jiang, B.; Liu, M.; Mao, M.; Mao, X. The first application of the Vogel-Fulcher-Tammann equation to biological problem: A new interpretation of the temperature dependent hydrogen exchanges rates of the thrombin-binding DNA. *Phys. Lett. A* **2007**, *361*, 248-251.

13. Angell, C.A.; Ngai, K.L.; McKenna, G.B.; McMillan, P.F.; Martin, S.W. Relaxation in glassforming liquids and amorphous solids. *J. Appl. Phys.* **2000**, *88*, 3113-3157.

14. Kokshenev, V.B. Characteristic temperatures of liquid-glass transition. *Physica A Stat. Mech. Appl.* **1999**, *262*, 88-97.

15. Takagi, Y.; Hosokawa, T.; Hoshikawa, K.; Kobayashi, H.; Hiki, Y. Relaxation of polystyrene near the glass transition temperature studied by acoustic measurements. *J. Phys. Soc. Jpn.* **2007**, *76*, 024604-024611.

16. Kivelson, D.; Tarjus, G.; Zhao, X.; Kivelson, S.A. Fitting of viscosity: Distinguishing the temperature dependences predicted by various models of supercooled liquids. *Phys. Rev. E* **1996**, *53*, 751-758.

17. Kivelson, D.; Tarjus, G. SuperArrhenius character of supercooled glass-forming liquids. *J. Non-Cryst. Solids* **1998**, *235-237*, 86-100.

18. Hecksher, T.; Nielsen, A.I.; Olsen, N.B.; Dyre, J.C. Little evidence for dynamic divergences in ultraviscous molecular liquids. *Nature Phys.* **2008**, *4*, 737-741.

19. Bässler, H. Viscous flow in supercooled liquids analyzed in terms of transport theory for random media with energetic disorder. *Phys. Rev. Lett.* **1987**, *58*, 767-770.

20. Angell, C.A. Relaxation in liquids, polymers and plastic crystals—Strong/fragile patterns and problems. *J. Non-Cryst. Solids* **1991**, *131-133*, 13-31.

21. Böhmer, R.; Ngai, K.L.; Angell, C.A.; Plazek, D.J. Nonexponential relaxations in strong and fragile glass formers. *J. Chem. Phys.* **1993**, *99*, 4201-4209.

22. Matsuoka, S. Entropy, free volume, and cooperative relaxation. *J. Res. Nat. Ins. Stand. Technol.* **1997**, *102*, 213-228.

23. Aniya, M. A model for the fragility of the melts. *J. Therm. Anal. Calorim.* **2002**, *69*, 971-978.

24. Aniya, M.; Shinkawa, T. A model for the fragility of metallic glass forming liquids. *Mater. Trans.* **2007**, *48*, 1793-1796.

25. Ndeugueu, J.L.; Ikeda, M.; Aniya, M. A comparison between the Bond Strength—Coordination Number Fluctuation model and the Random Walk model of viscosity. *J. Therm. Anal. Calorim.* **2010**, *99*, 33-38.

26. Aniya, M.; Ikeda, M. Viscosity of metallic glass forming liquids: Analysis based on Bond Strength-Coordination Number Fluctuations. *Mater. Sci. Forum* **2010**, *638-642*, 1621-1626.

27. Ikeda, M.; Aniya, M. Correlation between fragility and cooperativity in bulk metallic glass-forming liquids. *Intermetallics* **2010**, *18*, 1796-1799.

28. Ikeda, M.; Aniya, M. A model for the temperature dependence of the viscosity in Cu-As-Se system. *Solid State Ionics* **2009**, *180*, 522-526.

29. Adam, G.; Gibbs, J.H. On the temperature dependence of cooperative relaxation properties in glass-forming liquids. *J. Chem. Phys.* **1965**, *43*, 139-146.

30. Park, I.-S.; Saruta, K.; Kojima, S. Calorimetric and dielectric investigations of glass transition in intermediate glass-forming liquid. *J. Therm. Anal. Calorim.* **1999**, *57*, 687-693.

31. Yamamuro, O.; Ishikawa, M.; Kishimoto, I.; Pinvidic, J.-J.; Matsuo, T. Thermodynamic approach to glass transitions of plastically crystalline cyanoadamantane and isocyanocyclohexane. *J. Phys. Soc. Jpn.* **1999**, *68*, 2969-2976.

32. Cohen, M.H.; Grest, G.S. Liquid-glass transition, a free-volume approach. *Phys. Rev. B* **1979**, *20*, 1077-1098.

33. Haruyama, O.; Sakagami, H.; Nishiyama, N.; Inoue, A. The free volume kinetics during structural relaxation in bulk Pd-P based metallic glasses. *Mater. Sci. Eng. A* **2007**, *449-451*, 497-500.

34. Leyser, H.; Schulte, A.; Doster, W.; Petry, W. High-pressure specific-heat spectroscopy at the glass transition in *o*-terphenyl. *Phys. Rev. E* **1995**, *51*, 5899-5904.

35. Aniya, M.; Ikeda, M. Bond Strength—Coordination Number Fluctuations and the fragility of some ion conducting oxide and chalcogenide glass forming liquids. *Ionics* **2010**, *16*, 7-11.

36. Kohlrausch, R. Theorie des elektrischen Rückstander in der Leidener Flasche. *Pogg. Ann. Phys.* **1854**, *91*, 56-82.

37. Williams, G.; Watts, D.C. Non-symmetrical dielectric relaxation behavior arising from a simple empirical decay function. *Trans. Faraday Soc.* **1970**, *66*, 80-85.

38. Tanaka, H. Relationship among glass-forming ability, fragility, and short-range bond ordering of liquids. *J. Non-Cryst. Solids* **2005**, *351*, 678-690.

39. Novikov, V.N.; Sokolov, A.P. Poisson's ratio and the fragility of glass-forming liquids. *Nature* **2004**, *431*, 961-963.

40. Ngai, K.L. Dynamic and thermodynamic properties of glass-forming substances. *J. Non-Cryst. Solids* **2000**, *275*, 7-51.

41. Plazek, D.L.; Magill, J.H. Physical properties of aromatic hydrocarbons. IV. An analysis of the temperature dependence of the viscosity and the compliance of 1,3,5 tri-α-naphthylbenzene. *J. Chem. Phys.* **1968**, *49*, 3678-3682.

42. Kawamura, Y.; Inoue, A. Newtonian viscosity of supercooled liquid in a $Pd_{40}Ni_{20}P_{20}$ metallic glass. *Appl. Phys. Lett.* **2000**, *77*, 1114-1116.

43. Patkowski, A.; Paluch, M.; Gapiński, J. Relationship between T_0, T_g, and their pressure dependence for supercooled liquids. *J. Non-Cryst. Solids* **2003**, *330*, 259-263.

44. Zhao, Y.; Bian, X; Yin, K.; Zhou, J; Zhang, J.; Hou, X. Relations of the characteristic temperatures and fragility parameters in glass-forming metallic system. *Physica B Cond. Mat.* **2004**, *349*, 327-332.

45. Privalko, V.P. Glass transition in polymers: Dependence of the Kohlrausch-stretching exponent on the kinetic free volume fraction. *J. Non-Cryst. Solids* **1999**, *255*, 259-263.

46. Hodge, I.M. Strong and fragile liquids—A brief critique. *J. Non-Cryst. Solids* **1996**, *202*, 164-172.

47. Sidebottom, D.L.; Green, P.F.; Brow, R.K. Comparison of KWW and power law analyses of an ion-conducting glass. *J. Non-Cryst. Solids* **1995**, *183*, 151-160.

48. Schröter, K.; Donth, E. Comparison of shear response with other properties at the dynamic glass transition of different glassformers. *J. Non-Cryst. Solids* **2002**, *307-310*, 270-280.

49. Putz, K.; Green, P.F. Fragility in mixed alkali tellurites. *J. Non-Cryst. Solids* **2004**, *337*, 254-260.

50. Ngai, K.L.; Jonscher, A.K.; White, C.T. On the origin of the universal dielectric response in condensed matter. *Nature* **1979**, *277*, 185-189.

51. Vilgis, T.A. Strong and fragile glasses: A powerful classification and its consequences. *Phys. Rev. B* **1993**, *47*, 2882-2885.

52. Busch, R.; Bakke, E.; Johnson, W.L. Viscosity of the supercooled liquid and relaxation at the glass transition of the $Zr_{46.75}Ti_{8.25}Cu_{7.5}Ni_{10}Be_{27.5}$ bulk metallic glass forming alloy. *Acta Mater.* **1998**, *46*, 4725-4732.

53. Rault, J. Remarks on the Kohlrausch exponent and the Vogel-Fulcher-Tammann law in glass-forming materials. *J. Non-Cryst. Solids* **1999**, *260*, 164-166.

54. Wang, L.W.; Fecht, H.-J. A kinetic model for liquids: Relaxation in liquids, origin of the Vogel-Tammann-Fulcher equation, and the essence of fragility. *J. Appl. Phys.* **2008**, *104*, 113538-113547.

55. Trachenko, K. Slow dynamics and stress relaxation in a liquid as an elastic medium. *Phys. Rev. B* **2007**, *75*, 212201-212204.

56. Trachenko, K. The Vogel-Fulcher-Tammann law in the elastic theory of glass transition. *J. Non-Cryst. Solids* **2008**, *354*, 3903-3906.

57. Niss, K.; Dalle-Ferrier, C.; Tarjus, G.; Alba-Simionesco, C. On the correlation between fragility and stretching in glass-forming liquids. *J. Phys Cond. Matt.* **2007**, *19*, 076102-076126.